Vol 17 No 5, May 2008
1674-1056/2008/17(05)/1887-06

Chinese Physics B

© 2008 Chin. Phys. Soc.
and IOP Publishing Ltd

Characteristics of pentacene organic thin film transistor with top gate and bottom contact*

Yuan Guang-Cai(袁广才), Xu Zheng(徐 征)†, Zhao Su-Ling(赵谡玲), Zhang Fu-Jun(张福俊), Jiang Wei-Wei(姜薇薇), Song Dan-Dan(宋丹丹), Zhu Hai-Na(朱海娜), Li Shao-Yan(李少彦), Huang Jin-Ying(黄金英), Huang Hao(黄 豪), and Xu Xu-Rong(徐叙瑢)

Institute of Optoelectronic Technology, Beijing Jiaotong University, Beijing 100044, *China*
Key Laboratory of Luminescence and Optical Information (Beijing Jiaotong University), Ministry of Education, Beijing 100044, *China*

(Received 21 September 2007; revised manuscript received 12 October 2007)

High performance pentacene organic thin film transistors (OTFT) were designed and fabricated using SiO_2 deposited by electron beam evaporation as gate dielectric material. Pentacene thin films were prepared on glass substrate with S–D electrode pattern made from ITO by means of thermal evaporation through self-organized process. The threshold voltage V_{TH} was –2.75±0.1V in 0––50V range, and that subthreshold slopes were 0.42±0.05V/dec. The field-effect mobility (μ_{EF}) of OTFT device increased with the increase of V_{DS}, but the μ_{EF} of OTFT device increased and then decreased with increased V_{GS} when V_{DS} was kept constant. When V_{DS} was –50V, on/off current ratio was 0.48×10^5 and subthreshold slope was 0.44V/dec. The μ_{EF} was 1.10cm^2/(V·s), threshold voltage was –2.71V for the OTFT device.

Keywords: thin-film transistor, pentacene, threshold voltage, subthreshold slope
PACC: 7340, 7340L, 7360Q, 7340T

1. Introduction

Organic thin-film transistors (OTFTs) have recently attracted attention for its potential applications in smart cards, radio frequency identification tags and driving circuits for flat panel displays.[1,2] Meanwhile, particular attention has been paid to the morphology and energy level alignment of organic materials on different substrates.[3–6] The morphology and order of organic molecules strongly influence the charge carrier injection and transporting. Pentacene thin film transistors have shown different field effect mobilities for different substrates, e.g. 0.3 for SiO_2/Si, 1 for PMMA. Both organic and inorganic gate insulators can be used for OTFTs, the organic materials such as PVP (poly (4-vinylphenol)), PI (polyimide) are used as gate insulators for plastic displays due to the similar thermal expansion coefficients of the substrate and organic material layers.[7–11]

Ordinarily, Au is used as the source and drain electrodes in top gate OTFTs devices. Therefore, the interface energy and contact resistance between organic semiconductors and Au are of interest, since charges have to pass through the interface. Yet the research results of hole injection barriers (HIB) in pentacene/Au interfaces were controversial.[12,13] Similarly, contact resistance of source–drain and pentacene interface arises from mismatch of work functions and interaction between the metal electrode and the organic semiconductor.[14–16]

In this article, the characteristics of OTFT based on pentacene as active layer, including threshold voltage, mobility and sub threshold slope under different V_{GS} and V_{DS}, were studied in detail.

*Project supported by the National Natural Science Foundation of China (Grant No 60576016), the National High Technology Research and Development Program of China (Grant No 2006AA03Z0412), the Beijing Natural Science Foundation of China (Grant No 2073030), the National Grand Fundamental Research 973 Program of China (Grant No 2003CB314707), the National Natural Science Foundation of China (Grant No 10434030), the Excellent Doctor's Science and Technology Innovation Foundation of Beijing Jiaotong University of China (Grant No 48024).
†Corresponding author. E-mail: zhengxu@bjtu.edu.cn or ygc219@126.com

2. Experimental

We fabricated bottom contact pentacene OTFT with top gate structure on glass substrates. First, ITO S–D electrodes were deposited on the glass substrate. Then pentacene thin films were deposited on ITO S–D electrode as active layer. To obtain patterned pentacene islands we use thermal evaporation of a 98% purity commercial source in high vacuum of 2×10^{-3}Pa through self-organized process. The gate insulator layer SiO_2 was made by electron beam evaporation. Their thickness were 80nm (S–D electrodes ITO), and 100nm (pentacene), and 350nm (SiO_2), respectively. Finally, aluminium gate electrode of 110nm was deposited on gate insulator layer across shadow mask by thermal evaporation. All the thin films were prepared at low temperature (<100°C) and low deposition rate (≤0.06 nm). The $I-V$ measurements of the OTFTs were performed with a Keithley 2410 and 6430 Source Meter Parameter Analyser in darkness at room temperature.

The fabrication process indicated by cross-schematic structures, the bottom contact pentacene OTFT with top gate structure and the energy level diagram are shown in Figs.1(a), 1(b) and 1(c), respectively. The ratio of channel width to channel length, W/L of the pentacene OTFTs was chosen to be 10000μm/500μm.

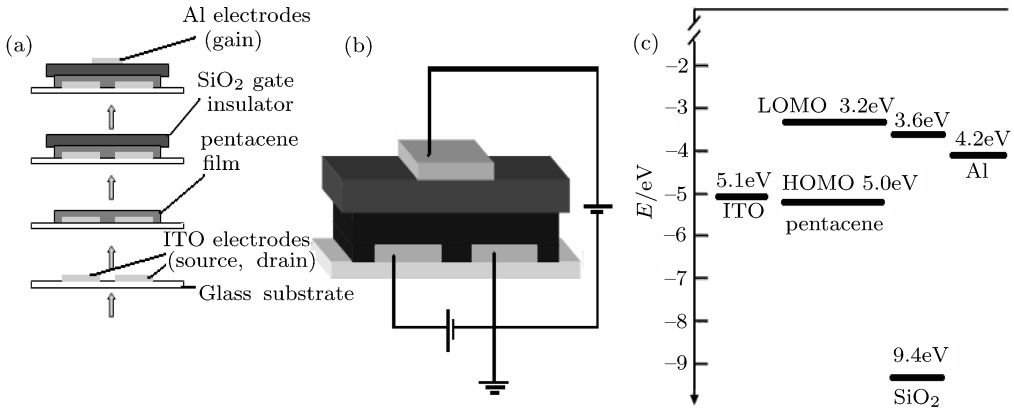


Fig.1. (a) The fabrication process shown by cross-schematic structures; (b) pentacene OTFT device with top gate structure; (c) energy level diagrams of ITO, pentacene, SiO_2, and metal (Al).

3. Results and discuss

Figure 2(a) shows the source–drain current (I_{DS}) versus source–drain voltage (V_{DS}) of the OTFT with ITO as the S–D electrodes at different gate voltages (V_{GS}). The device showed typical p-channel characteristics. As can be seen, the output characteristics displayed clear saturation currents which behaved as quadratic functions of the gate bias. The electrical transfer for the device is shown in Fig.2(b). Its unusual saturation behaviour is attributed to contact resistance on the source electrode. This is suggested by fitting of theoretical calculation to the experimental data in the linear regime of the I_{DS} vs V_{DS} plots of the output characteristics.[17−19]

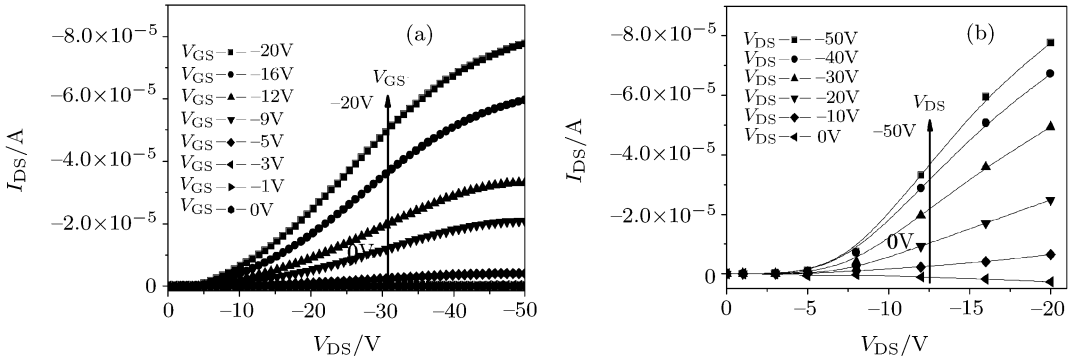


Fig.2. (a) Output characteristics and (b) transfer characteristics of OTFT device at different V_{GS} (–20V–0V) and V_{DS} (0V−−50V), respectively. The ratio of channel width to channel length W/L was 20.

The plots of $\log(I_{DS})$ vs V_{GS} and $\sqrt{I_{DS}}$ vs V_{GS} for OTFT devices with different V_{DS}: (a) V_{DS}=−50V, b) V_{DS}=–40V, (c) V_{DS}=–30V, (d) V_{DS}=–20, (e) V_{DS}=−10V are shown in Fig.3. Figure 3 shows the variation of field-effect mobility (μ_{EF}), threshold voltage (V_{TH}) , on/off current ratio and subthreshold slope of our fabricated OTFT with V_{GS}. We obtained field-effect mobility (μ_{EF}), threshold voltage (V_{TH}), on/off current radio, and subthreshold slope from $\log(I_{DS})$ vs V_{GS} and $\sqrt{I_{DS}}$ vs V_{GS} curves at different source to drain voltages V_{DS}.

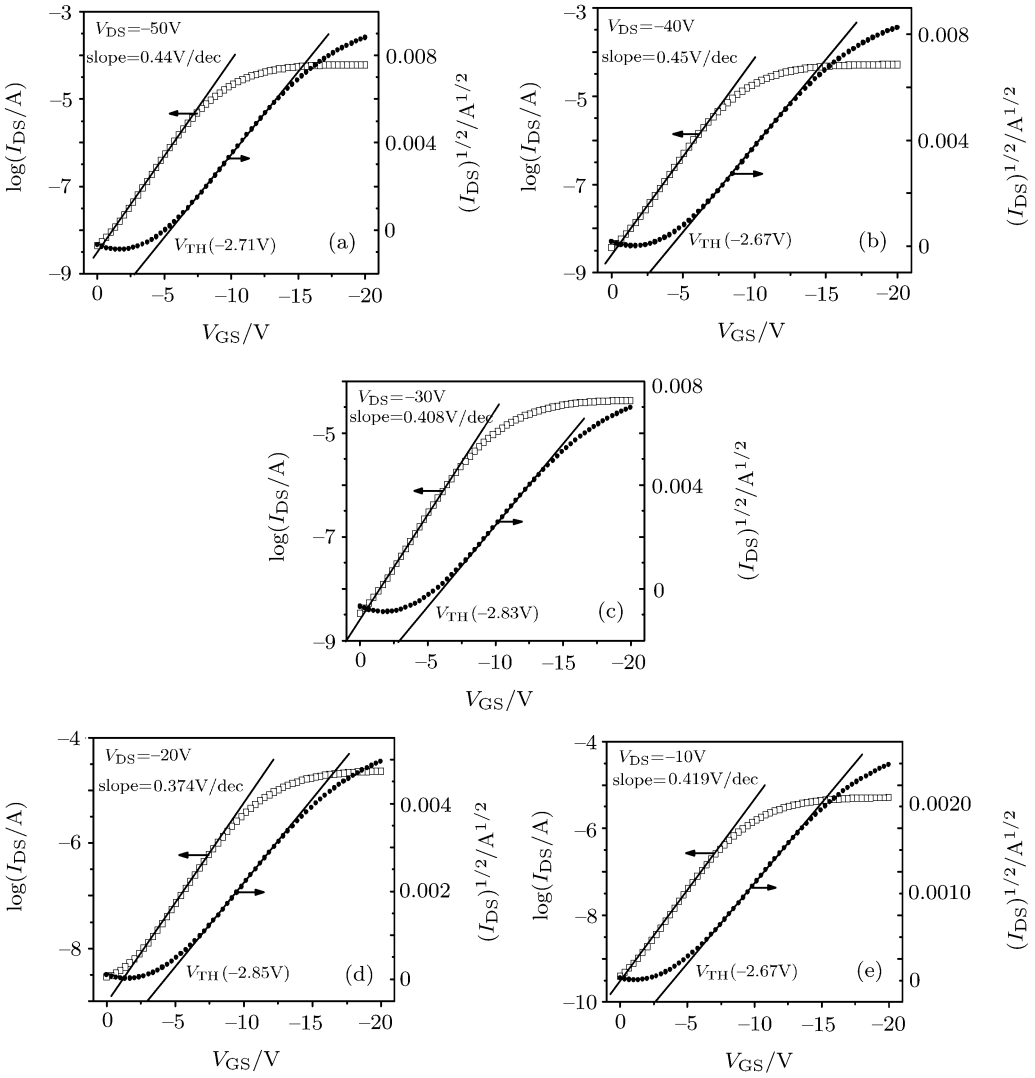


Fig.3. plots of $\log(I_{DS})$ vs V_{GS} and $\sqrt{I_{DS}}$ vs V_{GS} for OTFTs with different V_{ds}: (a) V_{ds}=–50V, (b) V_{ds}=–40V, (c) V_{ds}=–30V, (d) V_{ds}=–20, (e) V_{ds}=–10V.

In the linear regime $V_{DS} < (V_{GS} - V_T)$, the following expression is used to describe I_{DS}:

$$I_{DS} = \frac{W\mu_{EF}C_i}{L}\left[(V_{GS} - V_{TH})V_{DS} - \frac{V_{DS}^2}{2}\right], \qquad (1)$$

in which W is the transistor channel width, L is the transistor channel length, μ_{EF} is the field-effect mobility, V_{TH} is the threshold voltage, and C_i is the capacitance per unit area of the insulator.

In the saturation regime, $V_{DS} > (V_{GS} - V_T)$, I_D is given by

$$I_{DS} = \frac{WC_i\mu_{EF}}{2L}(V_{GS} - V_{TH})^2. \qquad (2)$$

The field-effect mobility in the linear regime was extracted from the transconductance of the device. If W, L and C_i are known, the field-effect mobility μ_{EF} was calculated at the linear regions from the following equation:

$$\mu_{EF} = \frac{L}{WC_iV_{DS}}\frac{\partial I_{DS}}{\partial V_{GS}}. \qquad (3)$$

It may be extracted also at large V_{GS}. The result may be better approximated than that of the mobility in the OTFT channel.

In the saturation regime $V_{DS} > (V_{GS} - V_{TH})$, the mobility was extracted from the transfer characteristics plotted as $\sqrt{I_{DS}}$ vs V_{GS}. The mobility is calculated using Eq.(3) by solving for μ_{EF},

$$\mu_{EF} = \frac{2L}{WC_i}\left(\frac{\partial\sqrt{I_{DS}}}{\partial V_{GS}}\right)^2. \quad (4)$$

The threshold voltage V_{TH} was determined from the intercept of the fitting line used to extract the mobility in the linear regime with x-axis or the intercept of the fitting line used to extract the mobility in the saturation regime with x-axis.[20−23]

The μ_{EF} and V_{TH} and on/off and subthreshold slope of OTFTs device were calculated for different V_{DS} in the linear and saturation regime by Eq.(3), Eq.(4), as shown in Table 1.

Table 1. Performance of bottom contact OTFTs with top gate structure in fixed V_{DS}.

V_{DS}/V	$K/10^{-4}$	V_{TH}/V	μ_{EF}/(cm^2/(V·s))	on/off(10^5)	subthreshold slope/(V/dec)
–50	3.32	–2.71	1.10	0.48	0.44
–40	3.11	–2.67	0.96	0.41	0.45
–30	2.62	–2.83	0.68	0.29	0.41
–20	1.84	–2.85	0.33	0.14	0.37
–10	0.94	–2.67	0.13	3.35	0.42

Note: $K = \partial\sqrt{I_D}/\partial V_{GS}$ (W/L=20, insulator layer SiO_2 (C_i=10nF/cm^2), $C_i = \varepsilon_0\varepsilon/d$, d is thickness of insulator layer)

Table 1 shows that the threshold voltage V_{TH} was –2.75±0.1V in 0−–50V range of V_{DS}, and that subthreshold slopes were 0.42±0.05V/dec for the OTFTs devices. The top contact OTFTs device with top gate structure is more stable, because insulator gate layer was deposited on active layer pentacene, and SiO_2 layer plays not only the important role of insulator layer, but also the role of passivation layer which protects the active layer from moisture and oxygen, which could induce degradation of OTFTs device, and consequently the stability of OTFTs devices was improved.[24]

Figure 3 and Table 1 show that the on/off current ratios of 0.48×10^5 and subthreshold slope of 0.44V/dec for OTFT device, which were also determined from the $\log(I_{DS})$ versus V_{GS} curve. At the same time, the field-effect mobility (μ_{EF}) of 1.10cm^2/(V·s), threshold voltage (V_{TH}) of –2.71V for the OTFT device were also determined from the $\sqrt{I_D}$ vs V_{GS} curve at fixed V_{DS} of –50V. Lower threshold voltage (–2.71V) indicates a low concentration of trap states and suggests the presence of barriers.[25] Indeed, the S-shaped output characteristics at small voltages indicate that even holes may experience small barriers before reaching the pentacene highest occupied molecular orbital (HOMO) level from the ITO electrodes.[26,27]

Table 2 shows the field-effect mobility μ_{EF} changing with V_{GS} when V_{DS} is definite for bottom contact OTFTs with top gate structure.

Figure 4(a) shows curves of threshold voltage vs V_{DS} and effective field-effect mobility vs V_{DS} for OTFT devices. We obtained more stable OTFTs device, the threshold voltage V_{TH} swing was ±0.1V in 0−–50V range of V_{DS}, and that subthreshold slopes has fluctuations of ±0.05V/dec. Figure 4(a) shows that the field-effect mobility (μ_{EF}) of OTFTs device increases with increasing V_{DS}, but the field-effect mobility (μ_{EF}) of OTFTs device increases and then decreases with increasing V_{GS} when V_{DS} was kept constant according to Fig.4(b).[28,29] For OTFT devices, there must be an optimization voltage value V_{GS} at which the field-effect mobility (μ_{EF}) has a maximum from our experiment results. This rule has already been verified in our experiments and the experimental result was shown in Table 2 and Fig.4.

Table 2. Experimental parameter of relation between field-effect mobility μ_{EF} and V_{GS} at definite V_{DS}.

V_{GS}/V	μ_{EF}/(cm^2/(V·s)) (V_{DS}=–10V)	μ_{EF}/(cm^2/(V·s)) (V_{DS}=–20V)	μ_{EF}/(cm^2/(V·s)) (V_{DS}=–30V)	μ_{EF}/(cm^2/(V·s)) (V_{DS}=–40V)	μ_{EF}/(cm^2/(V·s)) (V_{DS}=–50V)
–20V	0.694	0.708	0.707	0.694	0.697
–16V	0.895	0.919	0.917	0.895	0.90
–12V	1.001	1.047	1.043	1.010	1.016
–9V	1.194	1.275	1.260	1.194	1.210
–5V	0.774	0.909	0.893	0.774	0.80
–1V	0.046	0.222	0.138	0.046	0.059
0V	0.015	0.014	0.015	0.015	0.021

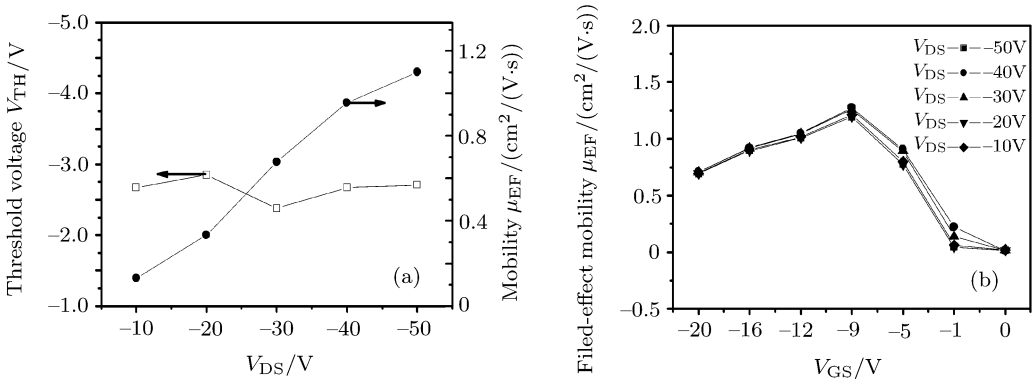


Fig.4. (a) Plots of threshold voltage V_{TH} vs V_{DS} and effective field-effect mobility μ_{EF} vs V_{DS}, and (b) Plots of effective field-effect mobility μ_{EF} vs V_{GS} in V_{DS} of 40V for pentacene based on OTFT devices with top gate structure.

4. Conclusion

We report studies of the V_{DS} and V_{GS} dependent carrier transport in pentacene OTFTs with top gate and top contact structure, which correlate the information about output and transfer characteristics. The pentacene films were deposited by thermal evaporation on glass substrate with ITO source and drain electrodes through a self-organized process. We obtained more stabile OTFTs device, the threshold voltage V_{TH} was –2.75±0.1V, in the 0––50V range of V_{DS}, and the subthreshold slopes were 0.42±0.05V/dec. The field-effect mobility (μ_{EF}) of OTFTs device increases with V_{DS} increasing, and the field-effect mobility (μ_{EF}) increases and then decreases with V_{GS} increasing at definite V_{DS}. When V_{DS} was –50V, the on/off current ratios of 0.48×10^5, subthreshold slope of 0.44V/dec, the field-effect mobility (μ_{EF}) of 1.10cm^2/(V·s) and threshold voltage (V_{TH}) of –2.71V for the OTFT device were obtained.

References

[1] Han S H, Kim J H, Janga J, Cho S M, Oh M H, Le S H and Choo D J 2006 *Appl. Phys. Lett.* **88** 073519

[2] Bana D, Han S, Lu Z H, Oogarah T, Spring Thorpe A J and Liu H C 2007 *Appl. Phys. Lett.* **90** 093108

[3] Zhang F J, Aollmer A, Zhang J, Xu Z, Rabe J P and Koch N 2007 *Organic Electronics* **8** 606

[4] Koch N and Vollmer A 2006 *Appl. Phys. Lett.* **89** 162107

[5] Cao Q J, Zhang Y M, Zhang Y M, Lu H L, Wang Y H, Chang Y C and Tang X Y 2007 *Chin. Phys.* **16** 1097

[6] Jiang T, Zhang H M, Wang W, Hu H Y and Dai X Y 2006 *Chin. Phys.* **15** 1339

[7] Hulea I N, Fratini S, Xie H, Mulder C L, Iossad N N, Rastelli G, Ciuchi S and Morpurgo A F 2006 *Nature Materials* **5** 982

[8] Halik M, Klauk H, Zschieschang U, Schmid G, Radlik W and Weber W 2002 *Adv. Mater.* **14** 1717

[9] Shtein M, Mapel J, Benziger J B and Forrest S R 2002 *Appl. Phys. Lett.* **81** 268

[10] Knipp D, Street R A, Volkel A and Ho J 2003 *J. Appl. Phys.* **93** 347

[11] Kelley T W, Boardman L D, Dunbar T D, Muyres D V, Pellerite M J and Smith T P 2003 *J. Phys. Chem.* B **107** 5877

[12] Koch N, Vollmer A, Duhm S, Sakamoto Y and Suzuki T 2007 *Adv. Mater.* **19** 112
[13] Zhao S Y, Wu C Y, Liu Z J, Li X D, Wang Z, Meng Z G, Xiong S Z and Zhang F 2006 *Acta Phys. Sin.* **55** 6095 (in Chinese)
[14] Luisier M, Schenk A and Fichtner W 2007 *Appl. Phys. Lett.* **90** 102103
[15] Halik M, Klauk H, Zschieschang U, Schmid G, Dehm C, Schütz M, Maisch S, Effenberger F, Brunnbauer M and Stellacci F 2004 *Nature* **431** 963
[16] Wang Y, Jia S, Chen Z J and Ji L J 2006 *Chin. Phys.* **15** 2297
[17] Liang W, Daniel Fine and Ananth Dodabalapurb 2004 *Appl. Phys. Lett.* **85** 6386
[18] Wang J, Wang H B, Yan X J, Huang H C and Yana D H 2005 *Appl. Phys. Lett.* **87** 093507
[19] Berliocchi1 M, Manenti1 M, Bolognesi1 A, Carlo1 A D, Lugli1 P, Paolesse R, Mandoy F, Natale C D, Proietti E and Petrocco G 2004 *Semicond. Sci. Technol.* **19** 354
[20] Schroeder R, Majewski L A and Grell M 2003 *Appl. Phys. Lett.* **83** 3201
[21] Zhang J, Wang J, Wang H B and Yana D H 2004 *Appl. Phys. Lett.* **84** 142
[22] Halik M, Klauk H, Zschieschang U, Schmid G, Radlik W, Ponomarenko S, Kirchmeyer S and Weber W 2003 *J. Appl. Lett.* **93** 2977
[23] Gundlach D J, Zhou L, Nichols J A, Jackson T N, Necliudovc P V and Shur M S 2006 *J. Appl. Lett.* **100** 024509
[24] Kim W J, Koo W H, Jo S J, Kim C S, Baika H K, Jiyoul L and Seongil I 2005 *J. Vac. Sci. Technol.* B **23** 2357
[25] Roy V A L, Zhi Y G, Xu Z X, Yu S C, Wai P, Chan H and Che C M 2005 *Adv. Mater.* **17** 1258
[26] Song D H, Choi M H, Kim J Y, Janga J and Kirchmeyer S 2007 *Appl. Phys. Lett.* **90** 053504
[27] da Silva Filho D A , Kim E-G and Bredas L-L 2005 *Adv. Mater.* **17** 1072
[28] Wang J, Yan X J, Xu Y X, Zhang J and Yana D H 2004 *Appl. Phys. Lett.* **85** 5424
[29] Vikram C Sundar, Jana Zaumseil, Vitaly Podzorov, Etienne Menard, Robert L Willett, Takao Someya, Michael E Gershenson and John A Rogers 2004 *Science* **303** 1644